OXIDIZED PHOSPHATIDYLCHOLINES FACILITATE PHOSPHOLIPID FLIP-FLOP IN LIPOSOMES.

Roman Volinsky †, Lukasz Cwiklik§‡, Piotr Jurkiewicz§, Martin Hof§, Pavel Jungwirth‡, and Paavo K.J. Kinnunen*†

†Helsinki Biophysics & Biomembrane Group, Department of Biomedical Engineering and Computational Science, Aalto University, Espoo, Finland

§ J. Heyrovsky Institute of Physical Chemistry, Academy of Sciences of the Czech Republic, v.v.i., Prague, Czech Republic

‡Institute of Organic Chemistry and Biochemistry, Academy of Sciences of the Czech Republic and Center for Biomolecules and Complex Molecular Systems, Prague, Czech Republic

RUNNING TITLE: Oxidized phospholipids and flip-flop

KEYWORDS: flip-flop, fluorescence, molecular dynamics, lipid bilayer, oxidation

* To whom correspondence should be addressed at Helsinki Biophysics & Biomembrane Group, *Department of Biomedical Engineering and Computational Science*, Aalto University, Espoo, Finland, paavo.kinnunen@aalto.fi

Abbreviations: ABC, ATP-binding cassette; Dtmac 4-[(*n*-dodecylthio)methyl]-7-(*N*,*N*-dimethylamino)-coumarine; ER, endoplasmic reticulum; Laurdan , 6-Lauroyl-2-dimethylaminonaphthalene; MD, molecular dynamic; P-C_6-NBD-PS 1- palmitoyl-2-[6-[(7-nitro-2-1,3-benzoxadiazol-4-yl)amino]hexanoyl]-*sn*-glycero-3-phospho-L-serine; Patman, 6-hexadecanoyl-2-(((2-(trimethylammonium)ethyl) methyl)-amino)naphthalene chloride; PazePC, 1-Palmitoyl-2-azelaoyl-sn-glycero-3-phosphocholine; PC, phosphatidylcholine; PE, phosphatidylethanol; PMF, potential of mean force; POPC 1-palmitoyl-2-oleyl-sn-glycero-3-phosphatidylcholine; POPS 1-palmitoyl-2-oleyl-sn-glycero-3-phospho-L-serine; PoxnoPC 1-palmitoyl-2-(9'-oxo-nonanoyl)-sn-glycero-3-phosphocholine; PS, phosphatidylserine; LUV, large unilamellar vesicles; ROS, reactive oxygen species; sn, stereochemical notation; SR, solvent relaxation; SUV, small unilamellar vesicles; TRES, time-resolved emission spectra;

Lipid asymmetry is a ubiquitous property of the lipid bilayers in cellular membranes and its maintenance and loss play important roles in cell physiology, such as blood coagulation and apoptosis. The resulting exposure of phosphatidylserine (PS) on the outer surface of the plasma membrane has been suggested to be caused by a specific membrane enzyme, 'scramblase, which catalyzes phospholipid flip-flop. In spite of extensive research the role of 'scramblase(s)' in apoptosis has remained elusive. Here we show that phospholipid flip-flop is efficiently enhanced in liposomes by oxidatively modified phosphatidylcholines. Combination of fluorescence spectroscopy and molecular dynamics simulations reveals that the mechanistic basis for this property of oxidized phosphatidylcholines is due to major changes imposed by the oxidized phospholipids on the biophysical properties of lipid bilayers, resulting in a fast cross bilayer diffusion of membrane phospholipids and loss of lipid asymmetry, requiring no 'scramblase' protein.

INTRODUCTION

Phospholipid asymmetry in biological membranes is essential for their proper function. Lipid transbilayer movement, maintaining this asymmetry, has been demonstrated for various cellular membranes (*1*), and is involved in processes such as biogenesis of endoplasmic reticulum (ER) (*2*), blood coagulation, and the clearance of apoptotic cells characterized by the exposure of phosphatidylserine (PS) on the outer leaflet of the plasma membrane (*3*). Lipid transport across cell membrane involves a combination of protein-mediated translocation and passive diffusion ('flip-flop'). The former has been shown to rely upon substrate specific ATPases: flippases (aminophospholipid translocases) and floppases (ATP-binding cassette, ABC transporters), responsible for establishing and maintenance of the transmembrane lipid asymmetry. The opposite, randomization of interleaflet lipid distribution has been assigned to ATP independent, nonspecific "scramblases" (4). While recent studies have implicated several protein candidates (5, 6), an affirmative identification of the scramblase and the triggering mechanisms remain perplexing (7, 8).

The passive transmembrane lipid diffusion is a very slow ($t_{1/2}$ of days and weeks), due to a high potential barrier (100-160 kJ/mol) for membrane permeability. (9) Large and/or charged headgroups and long saturated acyl chains have been shown to impede flip-flop. (10-12) Specifically, at least 10 fold decrease in flip-flop rates were reported for PC phospholipids over PE analogs and 2-fold decrease was found for every two methylene carbons added to the acyl chain at the *sn*-1 position. (10) On the other hand, defects in the lipid packing have been shown to provide lower energy pathways for the migration of polar lipids across the membrane. Thus, half-life times of minutes were reported for flip-flop in membranes with a high content of unsaturated lipids (13) and upon phase transition (14). Likewise, the presence of constituents effectively altering the membrane integrity such as addition of membrane spanning (15) or pore-forming (16) peptides has been shown to facilitate flip-flop.

One of the prominent apoptosis hallmarks - oxidative stress is associated with elevation in intracellular mitochondrial ROS (reactive oxygen species) production. (17, 18) Unsaturated lipids comprising the plasma membrane are particularly vulnerable to the oxidation. Although, processes involving in situ modification of lipid chemical structure can be readily expected to alternate the lipid molecule packing efficiency, impact of oxidative stress on lipid transbilayer movement has not been studied in detail.

In this study we followed after dynamic transbilayer distribution of the NBD-doped phosphatidylserine (PS) analogue that was determined using a dithionite-based assay. (19, 20) Our results indicate that the transbilayer movement of these analogs remarkably enhanced in the presence of oxidatively modified lipids. Solvent relaxation (SR) and molecular dynamic (MD) simulation analyses of the model system imparted by oxidized lipids, further attested to substantial changes in membrane lateral packing, enhanced water penetration and decrease in flip-flop energy barrier. Taken together our findings indicate a potential involvement of oxidative stress in lipid scrambling mechanisms.

MATERIALS AND METHODS

Materials

1-Palmitoyl-2-azelaoyl-sn-glycero-3-phosphocholine (PazePC), 1-palmitoyl-2-oleyl-sn-glycero-3-phosphatidylcholine (POPC), 1-palmitoyl-2-oleyl-sn-glycero-3-phospho-L-serine (POPS) 1-palmitoyl-2-(9'-oxo-nonanoyl)-sn-glycero-3-phosphocholine (PoxnoPC) and 1-palmitoyl-2-[6-[(7-nitro-2-1,3-benzoxadiazol-4-yl)amino]hexanoyl]-*sn*-glycero-3-phospho-L-serine (P-C_6-NBD-PS) were from Avanti Polar Lipids (Alabaster, AL). Phosphate Buffered Saline tablets, Hepes, sodium dithionite, and EDTA were from Sigma (St. Louis, MO). Concentrations of the nonfluorescent phospholipids were determined gravimetrically with a high-precision electrobalance (Cahn Instruments, Cerritos, CA). All buffers were prepared with deionized water that was glass distilled and purified further by a Milli-Q water system (Millipore Corp., Milford, MA). 4-[(*n*-dodecylthio)methyl]-7-(*N*,*N*-dimethylamino)-coumarin (Dtmac) was synthesized as described in (21) and purified by HPLC. 6-Lauroyl-2-dimethylaminonaphthalene (Laurdan), 6-hexadecanoyl-2-(((2-(trimethylammonium)ethyl) methyl)-amino)naphthalene chloride (Patman), 9-(9-anthroyloxy)stearic acid (9-AS), and 16-(9-anthroyloxy)palmitic acid (16-AP) were purchased from Invitrogen (Eugene, OR) and used without further purification.

Methods

Preparation of unilamellar vesicles

Lipid stock solutions were prepared in chloroform and mixed in this solvent to obtain the desired compositions. The solvent was removed under a stream of nitrogen and the lipid residue subsequently maintained under reduced pressure for at least 2 h. The dry lipid films were then hydrated at 25°C for 30 min in 10 mM phosphate buffer, 2.7 mM potassium chloride and 0.137 M sodium chloride, 0.1 mM EDTA, pH 7.4 to yield a final concentration of 250 μM. To assure efficient dispersion of the lipids the solutions were further placed in a bath-type sonicator for 20 min. During the above procedure the samples were vortexed several times, and minimal exposure to light was ensured. Subsequently, the dispersions were either sonicated using Covaris S2 (Covaris, Woburn, Ma, USA) to produce small unilamellar vesicles (SUV) or extruded through 100 nm polycarbonate track-etch membranes (Nucleopore, Whatman) in Lipex Extruder (Northern Lipids, Canada) to produce large unilamellar vesicles (LUV). To label vesicles exclusively on the outer-leaflet an appropriate

amount of NBD-labeled lipid analogue dissolved in methanol was added to the liposome solution to give final concentration of 1 mol% of total lipids. To obtain "symmetrically" labeled vesicles, the analogue was mixed with lipids before sonication or extrusion. The same procedure was used for preparation of LUV for solvent relaxation measurements, except that the NBD lipid analog was replaced by 1 mol% of one of polarity probes and the final lipid concentration in LUV suspension was 1 mM.

Dynamic light scattering measurements

Zetasizer Nano ZS (Malvern Instruments, Malvern, UK) was used to measure DLS for lipid dispersions in 10 x 10 mm disposable cuvettes. Data were analyzed with dedicated software provided by the instrument manufacturer. Temperature of the sample compartment was controlled by a Peltier element and set to 25°C. Average hydrodynamic diameters of 35 ± 4 nm and 100 ± 10 nm were obtained for SUVs and LUVs respectively.

Fluorescence measurements

Fluorescence measurements for the dithionite-quenching assay were made in the time-drive mode for 15 min. The measurements were conducted with a Perkin-Elmer (Foster City, CA) LS50B spectrofluorometer using 6.0 nm bandpasses for both the excitation and emission beams of 460 and 534 nm, respectively. Steady-state emission spectra and fluorescence decays for solvent relaxation method were recorded using Fluorolog 3 (Jobin Yvon) and IBH 5000 U SPC equipped with an IBH laser diode NanoLED 11 and a cooled Hamamatsu R3809U-50 microchannel plate photomultiplier, respectively.

Lipid transbilayer movement measurements

Outer leaflet labeled liposomes were used to measure the effect of the acyl chain composition of the host membrane on the rate of flip-flop of the P-C_6-NBD-PS probe. The translocation rates were calculated from the fluorescent signal intensity drop upon quenching of the P-C_6-NBD-PS remaining in the outer leaflet at various incubation time points (Fig. 1) and temperatures (19, 20).

Fluorescence solvent relaxation

For each sample a fluorescence emission spectrum and a series of fluorescence decays measured at emission wavelengths spanning the steady-state emission range were used to reconstruct time-resolved emission spectra (TRES) as described in (22). The position of TRES maximum, $\nu(t)$ reflects relaxation of the energy of the probe microenvironment. Starting from the Frank-Condon state at t = 0 the dipole molecules rearrange in response to the changed charge distribution around the fluorophore in order to minimize the free energy of the system. The energy drops exponentially reaching $\nu(\infty)$, which represents the dipolarily relaxed S1' state. The total red-shift of the TRES, given by: $\Delta\nu = \nu(0) - \nu(\infty)$, is a good measure of microenvironment polarity, which in model lipid membranes is strongly related to the extent of bilayer hydration.
The second parameter, integrated mean relaxation time, defined as

$$\tau = \int_0^\infty \frac{\nu(t) - \nu(\infty)}{\Delta\nu} dt, \qquad \text{Eq. 1}$$

describes the mobility of the polar environment of the fluorophore, which in lipid bilayer consist of hydrated lipid moieties.

Due to finite temporal resolution of the instrumentation, the TRES at t = 0, the so-called time-zero spectrum cannot be reconstructed from the measured decays, but has to be estimated using absorption and emission spectra measured in nonpolar solvent (e.g. cyclohexane) and absorption spectrum measured in the system of interest (23). Such estimates resulted in $\nu(0) = 22750$ for Dtmac and $\nu(0) = 23800$ cm-1 for Laurdan, Patman, 9-AS, and 16-AP. The shape and position of the time-zero spectrum was not affected by the addition of the oxidized lipids. Not only the two above defined parameters (i.e. $\Delta\nu$ and τ) were calculated, but detailed analysis of full width at half maximum of TRES was performed, see (24) for details. No discrepancies between τ and positions of FWHM(t) maxima were found. In order to prolong the relaxation processes to be within the temporal resolution of the instrumentation the SR measurements were performed at 10°C. This is particularly important for Dtmac, which accommodates at the level of the phosphate group of the lipid, where it experiences the most hydrated and mobile environment.

Molecular dynamics simulations

Simulations were performed for systems consisting in each case 64 lipid molecules (32 in each leaflet). As already shown by Tieleman and co-workers, a system of this size is large enough to provide well converged potentials of mean force for lipid flip-flop calculations. (25, 26) The non-oxidized system consisted of 63 POPC molecules and one POPS molecule, whereas in the oxidized bilayer six of randomly chosen POPC molecules were additionally exchanged for PoxnoPC. In each simulation more than 2700 water molecules were present, and a single sodium cation was placed in the water phase in order to neutralize the negative charge of the POPS molecule. The united-atom Berger's force-field was employed for lipid molecules (27) with additional parameters for the oxidized lipid taken from Tieleman et al. (28). Water molecules were described with the SPC model (29). Periodic boundary conditions were employed along with the semi-isotropic Parrinello-Ramhan barostat (30) with the pressure of 1 bar. The temperature of 310 K was controlled by the Nose-Hoover thermostat (31). Non-bonded interactions were calculated employing a cutoff of 1 nm, with the particle mesh Ewald method (32) accounting for long-range electrostatic forces. A time step of 2 fs was employed for integration of equations of motion. Calculations were performed with Gromacs 4.0.7 software (33).

For both non-oxidized and oxidized systems we started with a 10 ns equilibration followed by generation of initial configurations for umbrella sampling by pulling the phosphorous atom of the POPS molecule along the normal to the membrane (z-coordinate). For this we employed an umbrella potential with a force constant of 1000 kJ mol^{-1} nm^{-2} and with a pulling rate of 0.002 nm ps^{-1}. For both systems 27 initial configurations were chosen with a spacing of 0.1 nm in the position of the phosphorous atom with respect to the center of mass of the bilayer. For each of such umbrella sampling windows the z-coordinate of the phosphorus atom was restrained with a force constant of 3000 kJ mol^{-1} nm^{-2} and 10 ns equilibration runs were performed, each followed by a further 20 ns run. For each umbrella sampling window the values of the force acting on the restrained phosphorous atom of POPS in the z-direction during the production run were collected. Then, the weighted

histogram analysis method (34) was employed for calculating the potential of mean force (PMF), i.e., the changes of the free-energy.

On the timescale of the simulations phase separation between POPC and PoxnoPC was not observed. We also checked that the sodium counterion was residing in the water phase, i.e., not in direct contact with the anionic POPS.

RESULTS

Recently, we launched studies aiming at the characterization of the biophysical properties of lipid membranes imparted by oxidatively modified phospholipids (35), resulting from augmented oxidative stress, another hallmark of apoptosis. We concluded that oxidatively modified phosphatidylcholines can fluctuate between two extreme conformations, with the truncated chain a) inside the lipid bilayer and b) extended into the bulk aqueous phase (35), resulting in an increased penetration of water into the membrane, thus reducing the prevailing average hydrophobicity in the bilayer interior. These fluctuations and altered biophysical properties were subsequently verified in computer simulations (28, 36, 37). As the main barrier against transbilayer flip-flop of phospholipids is the hydrophobicity of the lipid bilayer hydrocarbon region, the introduction of oxidatively modified lipids with polar functional groups at the ends of truncated lipid acyl chains, can be readily expected to facilitate membrane permeability and the transbilayer movement of lipids. We tested this hypothesis by measuring lipid transmembrane diffusion with a fluorescence technique in liposomes containing oxidatively modified phosphatidylcholines, complemented by experimental determination of hydration profiles and MD simulations of such bilayers. The oxidized PCs (1-palmitoyl-2-azelaoyl-sn-glycero-3-phosphocholine, PazePC, and 1-palmitoyl-2-(9'-oxo-nonanoyl)-sn-glycero-3-phosphocholine, PoxnoPC, Fig. 2A) studied here represent oxidation products of some of the most abundant phospholipids of eukaryote membranes, i.e. polyunsaturated phosphatidylcholines bearing fatty acids with a *cis*-9 double bond (e.g. linoleic, or linolenic acid) in the *sn*-2 position.

Time-dependent changes in the transbilayer distribution of the fluorescent phosphotydilserine analogue, 1-palmitoyl-2-[6-[(7-nitro-2-1,3-benzoxadiazol-4-yl)amino]hexanoyl]-*sn*-glycero-3- phosphoserine (P-C_6-NBD-PS) were determined using a dithionite-quenching assay, converting NBD into a non-fluorescent derivative (19, 20), its translocation to the inner leaflet being monitored by the attenuation in the extent of decrease in fluorescence upon the external addition of dithionite (Fig. 1). The relative amounts of the above lipid analog in the outer leaflet of large unilamellar vesicles (LUV, d = 100 ± 10 nm) of varying lipid compositions were investigated (Fig. 2B). Pure POPC liposomes showed almost no flip-flop of the fluorescent PS ($t_{½}$ >two weeks), in keeping with previous results from e.g. neutron scattering (38). Interestingly, augmented flip-flop was evident in POPC LUV with X_{PazePC} = 0.10 ($t_{½}$ = 9 ± 1.2 h, Fig. 2B), while in POPC/PoxnoPC LUV ($X_{PoxnoPC}$ = 0.10) this 'scrambling' effect was not seen ($t_{½}$ > two weeks). The enhancement of PS flip-flop by these oxidatively modified phosphatidylcholines did depend on their content in bilayers. Accordingly, increasing X_{PazePC} to 0.14 or $X_{PoxnoPC}$ to 0.16 in POPC LUV resulted in greatly augmented probe flip-flop rates (with $t_{½}$ decreasing from > weeks to $t_{½}$ = 1.1 ± 0.15 h and $t_{½}$= 1.8 ± 0. 12 h, respectively, Fig. 2B). Further increase in the content of these oxidized lipids caused further deterioration of the membrane permeability barrier, with the addition of dithionite to POPC LUV with $X_{PazePC} \geq 0.20$ or $X_{PoxnoPC} \geq 0.20$ resulting in an immediate and complete quenching of the NBD fluorophore. As the permeability of dithionite through intact bilayers is very low, this is likely to indicate transient pore like defects to be induced at this content of the above oxidized phosphatidylcholines (39).

Oxidative stress in cells may involve phase separation and formation of domains exclusively populated by phospholipid oxidation products (35). The flip-flop rates measured in the presence of the above oxidized phosphatidylcholines did depend also on membrane curvature, with smaller contents of these phospholipids causing augmented transbilayer diffusion in small unilamellar vesicles (see Supplementary Material). The increase in probe

translocation rate is likely to emphasize the importance of conformational fluctuations of the oxidatively truncated phospholipid acyl chains, causing an increase in membrane penetration of water (35). The latter can be readily expected to diminish the free energy penalty for the mandatory step in the interleaflet phospholipid transfer, i.e., the transient accommodation of the phospholipid polar headgroup in the hydrophobic lipid bilayer hydrocarbon region. Further, this mechanism of increase in water permeation into bilayer caused by the conformational dynamics of oxidized phosphatidylcholine may well also underlie the enhanced flip-flop caused by detergents. Along these lines of reasoning the different efficiencies observed for a range of chemically divers detergents would then reflect their different efficiencies in increasing water permeation into lipid bilayers. (40) Notably, while the enhanced translocation rates described above were measured for NBD-PC, essentially similar data were obtained for NBD-labeled analogues (Fig. 3S), in keeping with the observed nonspecific nature of the scrambling (7).

In order to pursue on a more detailed level the relevant flip-flop promoting changes in the biophysical properties of lipid bilayers we conducted solvent relaxation (SR) fluorescence spectroscopy experiments addressing the effect of the above oxidatively modified PCs on the bilayer polarity profile, hydration, and mobility along the membrane normal using a series of probes located at different depths in phospholipid bilayers, viz. Dtmac, Laurdan, Patman, 9-AS, and 16-AP (Fig. 3S in the Supporting Material). Time-resolved emission spectra reconstructed from multiwavelength time-correlated single photon counting (TCSPS) measurements were analyzed in terms of time evolution of their positions and widths. The total time-dependent emission shift, $\Delta\nu$ is proportional to the polarity of the probe microenvironment (22), and relates to the depth-dependent hydration of the lipid bilayer in the vicinity of the fluorophore (24). The kinetics of the emission red-shift, characterized by the mean integrated relaxation time, τ (in nsec) reports on the mobility of the hydrated lipid moieties in the probe vicinity (24). The above parameters were recorded for POPC and oxPL-containing LUVs and are depicted as a function of the distance of the fluorophores from the bilayer center (Fig. 3). Because of the polarity/hydration profile of lipid membranes (41) the spectral shift, $\Delta\nu$ (for a given chromophore) becomes smaller and its mobility slower when approaching the non-hydrated bilayer interior. Notably, values of $\Delta\nu$ for all five probes in POPC LUV were: 2100, 3950, 3350, 2500, and 2350 cm^{-1} for Dtmac, Laurdan, Patman, 9-AS, and 16-AP, respectively. The obtained values for τ in POPC were as follows: Dtmac 1.17, Laurdan 3.12, and Patman 4.15 ns. Because the time-dependent red-shifts for 9-AS and 16-AP involve not only solvent relaxation but also intramolecular relaxation (42), an interpretation of the observed kinetics for these two probes in terms of their environment mobility would be ambiguous and was excluded from analysis. Changes in the total spectral shift ($\Delta\nu$), however, are informative, as both contributions (i.e. from solvent relaxation and from intramolecular relaxation) affect $\Delta\nu$ in the same way, i.e. increasing the spectral shift when the polarity of the environment increases.

The effects of 10 and 14 mol% of PazePC and 10 and 20 mol% of PoxnoPC on the measured polarity and mobility profiles in POPC bilayer are qualitatively similar (Fig. 3). Dtmac is most distant from the bilayer center, being accommodated near the phosphate group (43). Interestingly, Dtmac senses a slightly less hydrated and less mobile environment for membranes containing the oxidatively modified PCs, this effect being most pronounced for 14 mol% PazePC. The above data readily complies with the extended conformation being significant for PazePC, reducing the dielectricity at the membrane headgroup level. Laurdan and Patman have been shown to probe the hydration and mobility on the level of the sn-1 carbonyl moiety (44, 45). They both report increased hydration and a considerably

augmented mobility at the glycerol level of membranes containing the oxidized phospholipids. The impact on the probed mobility is largest for Patman, which is located ~ 0.1 nm deeper than Laurdan (44) and the effect increases with increasing oxPL content. In contrast, the augmented hydration is more pronounced for Laurdan; with the exception of POPC with 20 mol% of Poxno. When inspecting the time-dependent red-shifts of the 9-AS and 16-AP anthroyloxy chromophores located in the hydrocarbon region of the bilayer, the kinetic data reveal complex behavior, making detailed analysis ambiguous. 9-AS reports in all four oxPL-containing bilayers smaller $\Delta\nu$ values, thus suggesting that the polar moieties of the oxidatively truncated chains hinder the penetration of water into the vicinity of this chromophore residing in the hydrocarbon region of the bilayer. For 16-AP which is embedded in the center of the bilayer this effect is evident only for 10 mol% of PazePC. The overall relaxation behavior of these two hydrophobic probes reveals that the effects are considerably more pronounced for PazePC than for PoxnoPC.

The inherent perturbation brought into the system under study using fluorescent probes necessitates caution in data interpretation due to the fact that different fluorophores probe polarity with different sensitivity. Not only the absolute values of $\Delta\nu$, but also the relative values $\Delta\nu - \Delta\nu$ (POPC), should not be directly compared between different fluorophores. Meaningful comparison can be made only between AS-9 and AP-16, and between Laurdan and Patman probes. Nevertheless, the above SR experiments demonstrate a sinusoidal change in the membrane polarity profile to be introduced by both PazePC and PoxnoPC. The outer surface of the bilayer probed by Dtmac becomes less hydrated, in keeping with the expected reduced polarity of the aqueous phase adjacent to the phospholipid headgroup region caused by the extension of the truncated chains of PazePC and PoxnoPC into the aqueous phase vicinal to the lipid membrane surface. The adjacent glycerol backbone region (sensed by Patman and Laurdan) becomes more hydrated and mobile, while the center hydrocarbon region, accommodating 9-AS and 16-AS becomes dehydrated. The unexpected membrane hydrocarbon region dehydration observed for 10 mol% of PazePC, which is to a large extent absent at 14 mol% of PazePC, may indicate a local concentration dependent segregation of this oxidized phospholipid. Segregation could also promote the lateral partitioning of the anthroyl moiety bearing probes into regions enriched in saturated acyl chains. An additional factor may well be a shift in the conformational equilibrium of the oxidatively modified lipids because of steric factors and augmented packing in the hydrocarbon region containing the bulky chromophors.

To further elaborate the possible mechanisms of flip-flop enhancement induced by the above oxidized lipids, we characterized these membranes also by molecular dynamics (MD) simulations, comparing i) a membrane consisting of POPC only, and ii) a bilayer with 20 mol% of PoxnoPC in POPC. In both systems one POPC molecule was further replaced with a molecule of POPS, and the flip-flop of the latter at 310 K was studied. The potential of mean force (PMF) calculation employing the umbrella sampling method (46) was applied to obtain the free-energy barriers for the flip-flop of POPS in the above two membranes. PazePC was not investigated at this stage as the extent of protonation of the carboxylic acid moiety of the azelaoyl chain has not been determined and may vary depending on its immediate environment. Likewise, the effect of curvature (SUV vs LUV) was not addressed due to size limitations of MD simulations.

The energy barrier of phospholipid flip-flop across the bilayer results from a relocation into the hydrophobic interior of the membrane of the zwitterionic or, in the case of POPS, charged lipid headgroup, these polar moieties initially residing in contact with the

aqueous phase adjacent to the bilayer. The calculated free-energy profiles (Fig. 4A) correspond to the transfer of POPS molecule from one leaflet of the bilayer to the hydrophobic interior in the POPC vs. POPC/PoxnoPC membrane. Comparison of the free-energy curves and the total density profiles of the system and partial density profiles of water (Fig. 4B) demonstrates that the anionic headgroup of the POPS molecule preferentially resides in the vicinity of the headgroups of other lipids at a distance of about 2.2 nm from the bilayer center. During flip-flop, the hydrophilic headgroup of POPS has to enter the hydrophobic acyl chain region in the interior of the membrane, resulting in a free-energy penalty. The free-energy increases until the POPS headgroup reaches the center of the bilayer, whereafter it starts to diminish when the headgroup begins to approach the opposite leaflet of the bilayer, completing the flip-flop process. The maxima observed in both energy profiles (Fig. 4A) correspond to the free-energy barriers of the POPS flip-flop in POPC and POPC/PoxnoPC bilayers. In the non-oxidized membrane the energy barrier equals to 120 kJ/mol. This is a somewhat larger than the value calculated previously for membranes composed purely of zwitterionic PCs (25). Clearly, flip-flop for an anionic phospholipid is energetically more costly than for a zwitterionic one. The most important result of the present simulation is that the flip-flop free-energy cost for POPS in the oxidized POPC/PoxnoPC bilayer decreases by 20 kJ/mol to 100 kJ/mol. Converted to rates using a simple Arrhenius relation this means a 10^3 – 10^4 fold enhancement of the flip-flop rate due to phospholipid oxidation, which in perfect agreement with our observations with the fluorescence technique.

A detailed analysis of the MD trajectories also allowed for elucidation of the molecular mechanism of flip-flop of POPS. Representative snapshots depict typical stages observed during the transbilayer diffusion through the POPC/PoxnoPC membrane (Fig. 5). Initially, water defects (i.e., situations where water molecules penetrate into the bilayer) spontaneously form in the headgroup region of the membrane, assisted by the presence of PoxnoPC (Fig. 5A). As the anionic POPS headgroup enters the membrane interior, it is accompanied by water defects (Fig. 5B). As this process continues, the number of water molecules forming the defect increases. At the same time the POPS acyl chains undergo profound conformational changes (Fig. 5C). As the POPS headgroup reaches the center of the bilayer a transient water pore is formed across the membrane, stabilized by PoxnoPC. At this point, the POPS acyl chains become oriented parallel to the surface of the membrane in the center of the bilayer (Fig. 5D). As the POPS headgroup crosses the membrane center, the water pore disappears. Water defects originating from the opposite leaflet start to form around the POPS headgroup, again aided by PoxnoPC from that leaflet (Fig 5E). Subsequently, acyl chains of the POPS molecule reorient perpendicular to the membrane surface (Fig. 5F), pointing their ends into the center of the bilayer. Flip-flop in a non-oxidized bilayer exhibits analogous phases as above for an oxidized membrane, except that there is no PoxnoPC to facilitate the formation of the water filled defects. The crucial role of water pores in flip-flop was recently emphasized in a different context of defects formed by ionic gradient across the membrane (47). In summary, the presence of 20 % of PoxnoPC in the POPC membrane decreases the free energy barrier for POPS flip-flop by 20 ± 5 kJ/mol, with contributions to this decrease in the free energy penalty from several mechanisms. First, PoxnoPC assists in the creation and stabilization of water defects in the headgroup region of the membrane. Second, the oxidized lipids stabilize the transient water pores, which are formed during the flip-flop process.

DISCUSSION

PoxnoPC has been recognized as the main product of ozone mediated oxidation of lung surfactant extracts, with apoptosis and necrosis promoting activity (48), similarly to PazePC (49). Our current findings are in agreement with the effects on cultured cells and isolated mitochondria of PazePC and its 1-alkyl- analog HazePC (1-hexadecyl-2-azelaoyl-sn-glycero-3-phosphocholine)(50). The latter is an 1-alkyl analog and resistant to hydrolysis by phospholipases A1 and on a molar basis twice as efficient as PazePC in inducing apoptosis. Accordingly, the addition of micromolar concentrations of these lipids to cultured cells causes apoptosis with rapid non-receptor dependent exposure of PS. Further, these lipids become concentrated into mitochondria and were shown to depolarize isolated mitochondria and cause permeability transition assisted by the proapoptotic Bid and counteracted by the antiapoptotic Bcl-XL. (49). These effects were reversible upon scavenging of these oxidized lipids by added BSA. The total phospholipid content of cultured cells exposed to HazePC was measured as approx. 15 μmoles phosphate per 10^6 cells (50) while HazePC was found in picomolar levels. In this context it is worth recognizing that mitochondria are the main source of ROS and are thus likely to initially have also the highest total content of oxidized phospholipids. Together with the high protein/lipid ratio in mitochondria, the local concentrations of oxidized phospholipids in these bilayers are likely to readily reach values (10 mol%) sufficient to facilitate phospholipid scrambling. Along these lines Kagan and coworkers demonstrated an accumulation of oxidized phosphatidylserine in the plasma membrane of cultured cells and stimulated scrambling of non-oxidized PS and PE (51). As no inhibition of aminophospholipid translocase by oxidized phosphatidylserine was detected these authors suggested this lipid to act in a non-enzymatic fashion. However, these experiments employed cultured cells, making mechanistic conclusions ambiguous.

Our present results conclusively demonstrate for the first time that a loss of lipid asymmetry can be solely caused by altered biophysical properties of the lipid bilayer imparted by the oxidized phospholipids, making participation of a ‘scramblase’ protein in lipid translocation unnecessary. However, caution is needed in relating our findings to the situation prevailing in biological membranes in vivo, because a significant fraction of cellular membrane area is occupied by transmembrane proteins, which have a profound impact on the conformational dynamics of their vicinal lipids. Accordingly, the characterization of the detailed effects of oxidized lipids in vivo is a formidable challenge. As an example, the local membrane concentrations of oxidized phospholipids in vivo are likely to vary significantly, in keeping with the inherent fluctuations of biomembranes representing many body systems (52). Nevertheless, our findings, derived from fluorescence spectroscopy and molecular dynamics simulations of a well-defined model biomembrane system reveal, that oxidative attack on membrane phospholipids could represent a causative factor inducing as such the loss of phospholipid asymmetry in apoptosis and cancer, resulting in the exposure of phosphatidylserine on the outer surface of the affected cells. Further along these lines we are currently investigating more complex model membranes, approaching the composition of cellular membranes.

SUPPORTING MATERIAL

Two sections, references and two figures are available at http://www.biophysj.org/biophysj/supplemental/

ACKNOWLEDGEMENTS

We thank Drs. Stephen White and Doug Tobias (UCI) for valuable comments and Dr. Tom McIntyre (Department of Cell Biology, Cleveland Clinic, Cleveland, Ohio) for communicating to us the phospholipid concentrations of cultured cells exposed to oxidized phosphatidylcholines. This study was financed by the Finnish Academy and the Czech Science Foundation (ESF EUROMEMBRANE project MEM/09/E006). HBBG is further supported by grants from the Sigrid Juselius Foundation. PJ and MH acknowledges support from the Czech Ministry of Education (grant LC 512 512 and grant LC06063, respectively), the Czech Science Foundation (grant 203/08/0114), and the Academy of Sciences (Praemium Academie).

REFERENCES

1. Leventis, P. A., and S. Grinstein. 2010. The distribution and function of phosphatidylserine in cellular membranes. Annu Rev Biophys 39:407-427.
2. Higgins, J. A. 1981. Biogenesis of endoplasmic reticulum phosphatidylcholine: Translocation of intermediates across the membrane bilayer during methylation of phosphatidylethanolamine. Biochim. Biophys. Acta, Biomembr. 640:1-15.
3. Tanaka, Y., and A. J. Schroit. 1983. Insertion of fluorescent phosphatidylserine into the plasma membrane of red blood cells. Recognition by autologous macrophages. J. Biol. Chem. 258:11335-11343.
4. Williamson, P., A. Kulick, A. Zachowski, R. A. Schlegel, and P. F. Devaux. 1992. Ca2+ Induces Transbilayer Redistribution of all Major Phospholipids in Human Erythrocytes. Biochemistry 31:6355-6360.
5. Fadeel, B., and D. Xue. 2009. The ins and outs of phospholipid asymmetry in the plasma membrane: roles in health and disease Cr. Rev. Biochem. Mol. Biol. 44:264-277.
6. Suzuki, J., M. Umeda, P. J. Sims, and S. Nagata. 2010. Calcium-dependent phospholipid scrambling by TMEM16F. Nature 468:834-838.
7. van Meer, G., and D. R. F. Voelker, Gerald W. 2008. Membrane lipids: where they are and how they behave. Nat Rev Mol Cell Bio 9:112-124.
8. Williamson, P., and R. A. Schlegel. 2002. Transbilayer phospholipid movement and the clearance of apoptotic cells. Biochim Biophys Acta 1585:53- 63.
9. John, K., S. Schreiber, J. Kubelt, A. Herrmann, and P. Muller. 2002. Transbilayer Movement of Phospholipids at the Main Phase Transition of Lipid Membranes: Implications for Rapid Flip-Flop in Biological Membranes. Biophysical Journal 83:3315-3323.
10. Homan, R., and H. J. Pownall. 1988. Transbilayer diffusion of phospholipids: dependence on headgroup structure and acyl chain length. Biochim. Biophys. Acta, Biomembr. 938:155-166.
11. Kornberg, R. D., and H. M. McConnell. 1971. Inside-outside transitions of phospholipids in vesicle membranes. Biochemistry 10:1111-1120.
12. Anglin, T. C., and J. C. Conboy. 2009. Kinetics and Thermodynamics of Flip-Flop in Binary Phospholipid Membranes Measured by Sum-Frequency Vibrational Spectroscopy. Biochemistry 48:10220-10234.
13. Armstrong, V. T., M. R. Brzustowicz, S. R. Wassall, L. J. Jenski, and W. Stillwell. 2003. Rapid flip-flop in polyunsaturated (docosahexaenoate) phospholipid membranes. Archives of Biochemistry and Biophysics 414:74-82.
14. De Kruijff, B., and E. J. J. Van Zoelen. 1978. Effect of the phase transition on the transbilayer movement of dimyristoyl phosphatidylcholine in unilamellar vesicles. Biochim. Biophys. Acta, Biomembr. 511:105-115.
15. Kol, M. A., A. I. P. M. de Kroon, D. T. S. Rijkers, J. A. Killian, and B. de Kruijff. 2001. Membrane-spanning peptides induce phospholipid flop: A model for phospholipid translocation across the inner membrane of E. coli. Biochemistry 40:10500-10506.
16. Matsuzaki, K., O. Murase, N. Fujii, and K. Miyajima. 1996. An antimicrobial peptide, magainin 2, induced rapid flip-flop of phospholipids coupled with pore formation and peptide translocation. Biochemistry 35:11361-11368.
17. Newmeyer, D. D., and S. Ferguson-Miller. 2003. Mitochondria, releasing power for life and unleashing the machineries of death. Cell 112:481-490.
18. Simon, H.-U., A. Haj-Yehia, and F. Levi-Schaffer. 2000. Role of reactive oxygen species (ROS) in apoptosis induction. Apoptosis 5:415-418.
19. Angeletti, C., and J. W. Nichols. 1998. Dithionite Quenching Rate Measurement of the Inside-Outside Membrane Bilayer Distribution of 7-Nitrobenz-2-oxa-1,3-diazol-4-yl-Labeled Phospholipids. Biochemistry 37:15114-15119.

20. McIntyre, J. C., and R. G. Sleight. 1991. Fluorescence assay for phospholipid membrane asymmetry. Biochemistry 30:11819-11827.
21. Sterk, G. J., P. A. Thijsse, R. F. Epand, H. W. Wong Fong Sang, R. Kraayenhof, and R. M. Epand. 1997. New fluorescent probes for polarity estimations at different distances from the membrane interface. J. Fluoresc. 7:115S-118S.
22. Horng, M. L., J. A. Gardecki, A. Papazyan, and M. Maroncelli. 1995. Subpicosecond Measurements of Polar Solvation Dynamics - Coumarin-153 Revisited. J Phys Chem 99:17311-17337.
23. Fee, R. S., and M. Maroncelli. 1994. Estimating the time-zero spectrum in time-resolved emission measurements of solvation dynamics. Chem. Phys. 183:235-247.
24. Jurkiewicz, P., J. Sykora, A. Olzynska, J. Humplickova, and M. Hof. 2005. Solvent relaxation in phospholipid bilayers: Principles and recent applications. J. Fluoresc. 15:883-894.
25. Sapay, N., W. F. D. Bennett, and D. P. Tieleman. 2009. Thermodynamics of flip-flop and desorption for a systematic series of phosphatidylcholine lipids Soft Matter 5:3295– 3302
26. Tieleman, D. P., and S.-J. Marrink. 2006. Lipids out of equilibrium: Energetics of desorption and pore mediated flip-flop. . J. Am. Chem. Soc. 128:12462-12467
27. Berger, O., O. Edholm, and F. Jahnig. 1997. Molecular dynamics simulations of a fluid bilayer of dipalmitoylphosphatidylcholine at full hydration, constant pressure, and constant temperature Biophys. J. 72:2002-2013.
28. Wong-ekkabut, J., Z. Xu, W. Triampo, I.-M. Tang, D. P. Tieleman, and L. Monticelli. 2007. Effect of Lipid Peroxidation on the Properties of Lipid Bilayers: A Molecular Dynamics Study. Biophys J. 93:4225-4236.
29. Berendsen, H. J. C., J. P. M. Postma, W. F. van Gunsteren, and J. Hermans. 1981. In Intramolecular Forces. B. Pullman, editor. D. Reidel Publishing Company, Dordrecht. 331-342.
30. Parrinello, M., and A. Rahman. 1981. Polymorphic transitions in single crystals: A new molecular dynamics method. J . Appl. Phys. 52:7182-7190.
31. Hoover, W. G. 1985. Canonical dynamics: Equilibrium phase-space distributions. Phys. Rev. A 31:1695–1697.
32. Darden, T., D. York, and L. Petersen. 1993. Particle mesh Ewald: An N-log(N) method for Ewald sums in large systems. J. Chem. Phys. 98:10089-10092.
33. Hess, B., C. Kutzner, D. van der Spoel, and E. Lindhal. 2008. GROMACS 4: Algorithms for Highly Efficient, Load-Balanced, and Scalable Molecular Simulation. J. Chem. Theory Comput. 4:435–447
34. Kumar, S., J. M. Rosenberg, D. Bouzida, R. H. Swendsen, and P. A. Kollman. 1992. The weighted histogram analysis method for free-energy calculations on biomolecules. I. The method. J. Comp. Chem . 13:1011-1021.
35. Sabatini, K., J.-P. Mattila, F. M. Megli, and P. K. J. Kinnunen. 2006. Characterization of two oxidatively modified phospholipids in mixed monolayers with DPPC. Biophys. J. 90:4488-4499.
36. Beranova, L., L. Cwiklik, P. Jurkiewicz, M. Hof, and P. Jungwirth. 2010. Oxidation Changes Physical Properties of Phospholipid Bilayers: Flueorescence Spectroscopy and Molecular Simulations. Langmuir 26:6140-6144.
37. Cwiklik, L., and P. Jungwirth. 2010. Massive oxidation of phospholipid membranes leads to pore creation and bilayer disintegration Chem. Phys. Letters 486:99-103.
38. Nakano, M., M. Fukuda, T. Kudo, N. Matsuzaki, T. Azuma, K. Sekine, H. Endo, and T. Handa. 2009. Flip-Flop of Phospholipids in Vesicles: Kinetic Analysis with Time-Resolved Small-Angle Neutron Scattering. J. Phys. Chem. B 113:6745-6748.
39. Langner, M., and S. W. Hui. 1993. Dithionite penetration through phospholipid bilayers as a measure of defects in lipid molecular packing. Chem. Phys. Lipids 65:23-30.

40. Pantaler, E., D. Kamp, and C. W. M. Haest. 2000. Acceleration of phospholipid flip-flop in the erythrocyte membrane by detergents differing in polar head group and alkyl chain length. Biochim. Biophys. Acta 1509 397-408.
41. White, S. H., and W. C. Wimley. 1998. Hydrophobic interactions of peptides with membrane interfaces. Biochim. Biophys. Acta-Rev. Biomembr. 1376:339-352
42. Sykora, J., P. Slavicek, P. Jungwirth, J. Barucha, and M. Hof. 2007. Time-dependent stokes shifts of fluorescent dyes in the hydrophobic backbone region of a phospholipid bilayer: Combination of fluorescence spectroscopy and ab initio calculations. J. Phys. Chem. B 111:5869-5877.
43. Sykora, J., P. Jurkiewicz, R. M. Epand, R. Kraayenhof, M. Langner, and M. Hof. 2005. Influence of the curvature on the water structure in the headgroup region of phospholipid bilayer studied by the solvent relaxation technique. Chem. Phys. Lipids 135:213-221.
44. Jurkiewicz, P., A. Olzynska, M. Langner, and M. Hof. 2006. Headgroup hydration and mobility of DOTAP/DOPC bilayers: A fluorescence solvent relaxation study. Langmuir 22:8741-8749.
45. Olzynska, A., A. Zan, P. Jurkiewicz, J. Sykora, G. Grobner, M. Langner, and M. Hof. 2007. Molecular interpretation of fluorescence solvent relaxation of Patman and H-2 NMR experiments in phosphatidylcholine bilayers. Chem. Phys. Lipids 147:69-77
46. Torrie, G. M., and J. Valleau. 1977. J. Comp. Phys. 23:187.
47. Gurtovenko, A. A., and I. Vattulainen. 2007. Molecular Mechanism for Lipid Flip-Flops. J. Phys. Chem. B 111:13554-13559.
48. Uhlson, C., K. Harrison, C. B. Allen, S. Ahmad, C. W. White, and R. C. Murphy. 2002. Oxidized phospholipids derived from ozone-treated lung surfactant extract reduce macrophage and epithelial cell viability. Chem. Res. Toxicol. 15:896-906.
49. Chen, R., A. E. Feldstein, and T. M. McIntyre. 2009 Suppression of Mitochondrial Function by Oxidatively Truncated Phospholipids Is Reversible, Aided by Bid, and Suppressed by Bcl-XL. J. Biol. Chem. 284:26297-26308.
50. Chen, R., L. Yang, and T. M. McIntyre. 2007. Cytotoxic Phospholipid Oxidation Products Cell Death From Mitochondrial Damage And The Intrinsic Caspase Cascade. The Journal of Biological Chemistry 282:24842-24850.
51. Tyurina, Y. Y., V. A. Tyurina, Q. Zhaoa, M. Djukica, P. J. Quinnd, B. R. Pitta, and V. E. Kagan. 2004. Oxidation of phosphatidylserine: a mechanism for plasma membrane phospholipid scrambling during apoptosis? Biochem. Biophys. Res. Comm. 324 1059-1064.
52. Mouritsen, O. G., and P. J. K. Kinnunen. 1996. Role of lipid organization and dynamics for membrane functionality. In Membrane Structure and Dynamics. A Molecular Perspective from Computation and Experiment. K. M. Mertz Jr., and B. Roux, editors. Birkhäuser Publ. Co. 463-502.

FIGURE LEGENDS

Fig. 1. Flip-flop assay of P-C_6-NBD-PS in POPC/PazePC (8.9:1 mole ratio) SUV. Methanol solution of P-C_6-NBD-PS was added to POPC/PazePC SUV to give 1% of total phospholipid concentration. Following incubation at 37°C, aliquots of 1 ml of 250μM SUV suspension were taken at various times: a) 2h 30 min, b) 5 h 20 min, c) 10 h 30 min, d) 26h 30 min, and added to stirred spectrofluorometer cuvette containing 1 ml PBS buffer (pH 7.4). Immediately following stabilization of the fluorescence trace 8 μl of 0.6 M dithionite (pH 10) were added to quench fluorophore molecules in the outer leaflet. Following completion of the fluorescence quenching, 25 μl of 10% Triton X-100 were added to allow access to the translocated probes.

Fig. 2. (**A**) Chemical structures of the oxidized phospholipids used: 1-palmitoyl-2-azelaoyl-sn-glycero-3-phosphocholine (PazePC), 1-palmitoyl-2-(9'-oxo-nonanoyl)-sn-glycero-3-phosphocholine (PoxnoPC). (**B**) Time-dependent decrease in the outer leaflet fraction of P-C_6-NBD-PS in LUVs consisting of purePOPC (■), POPC/PoxnoPC (8.9:1 mole ratio, ●), POPC/PazePC (8.9:1 mole ratio, ▲), POPC/PoxnoPC (8.3:1.6 mole ratio, ⬟), and POPC/PazePC (8.5:1.4 mole ratio, ▼) at 37°C.

Fig. 3. Fluorescence solvent relaxation parameters: relative integrated relaxation time (A) and differences in spectral shift (B), normalized relative to the values obtained for pure POPC (given in text). Probes are shown at their positions known from literature (see the text). For the sake of clarity of presentation the position of Laurdan has been shifted by 0.1 nm outward from Patman.

Fig. 4. (A) Free energy profiles, exemplifying barrier for POPS entering either non-oxidized (POPC) or oxidized (4:1 POPC:PoxnoPC) membrane, as a function of the POPS-phosphate group distance to the bilayer center. The width of the curves represents statistical error estimated using shorter sub-blocks of the corresponding MD trajectories. **(B)** Total density profiles of the system and partial density profiles of water for both non-oxidized and oxidized bilayer.

Fig. 5. Selected snapshots depicting the progress of flip-flop of the oxidized membrane by a POPS molecule in the potential of mean force calculations. Color coding: O-atoms (pink) and H-atoms (gray) of water, PoxnoPC lipids (yellow), POPS acyl chains (blue), and O-atoms of the carboxylic group of POPS headgroup (red).

FIGURES

Figure. 1

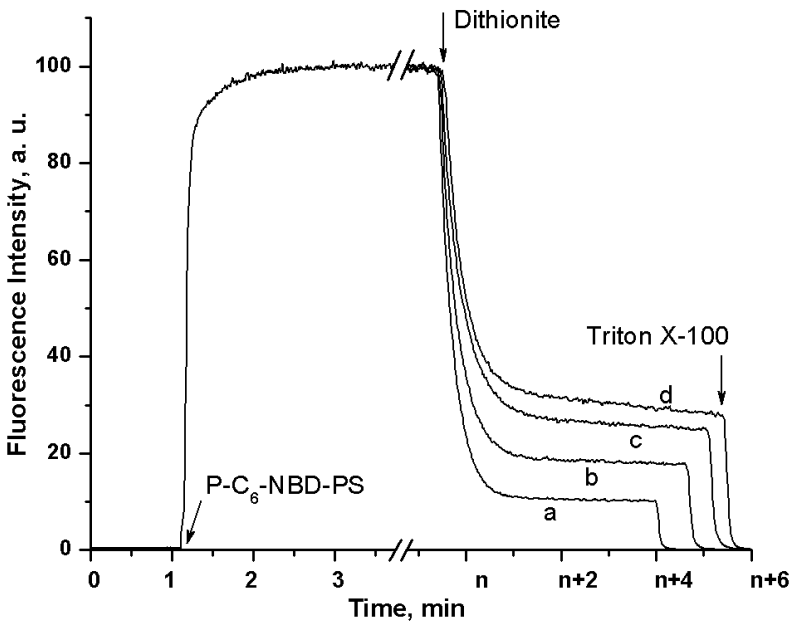

Figure 2

A

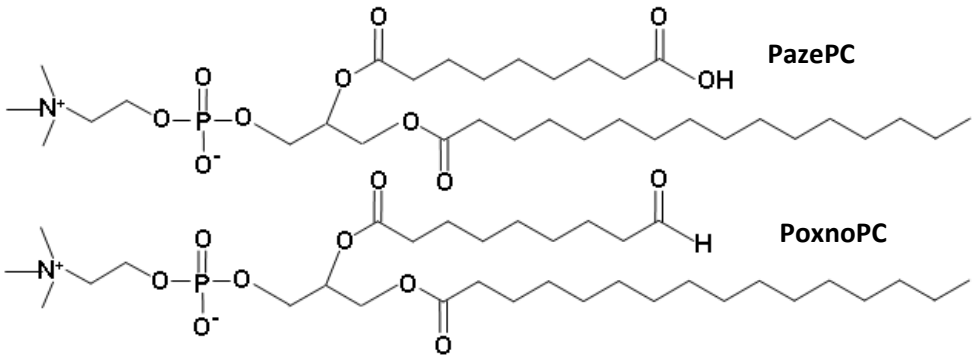
PazePC
PoxnoPC

B

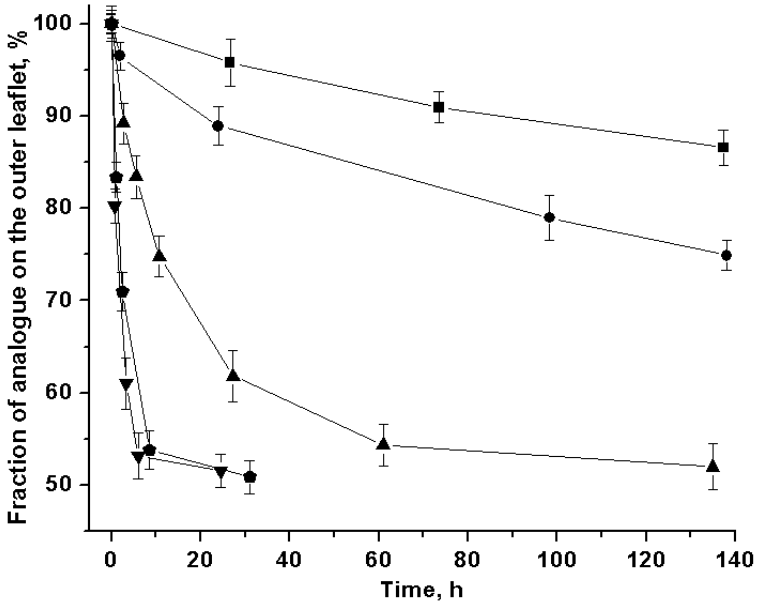
Fraction of analogue on the outer leaflet, %
100
90
80
70
60
50
0
20
40
60
80
100
120
140
Time, h

Figure 3

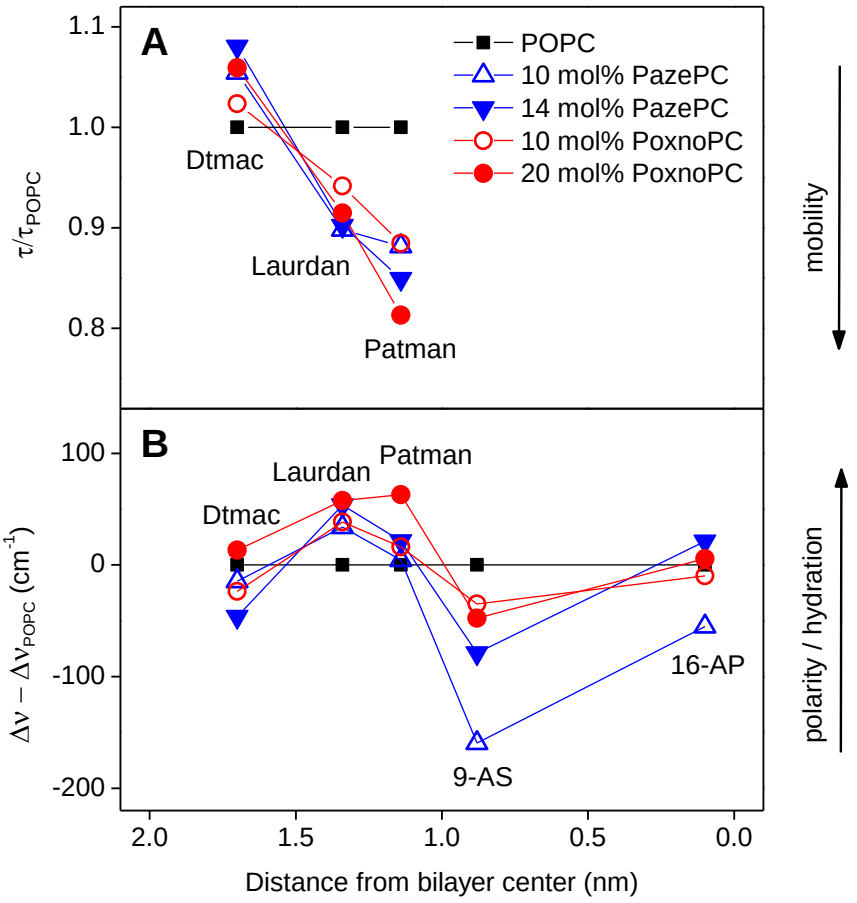
A
B
POPC
10 mol% PazePC
14 mol% PazePC
10 mol% PoxnoPC
20 mol% PoxnoPC
Dtmac
Laurdan
Patman
9-AS
16-AP
τ/τPOPC
Δν – ΔνPOPC (cm-1)
Distance from bilayer center (nm)
mobility
polarity / hydration
1.1
1.0
0.9
0.8
100
0
-100
-200
2.0
1.5
1.0
0.5
0.0

Figure 4

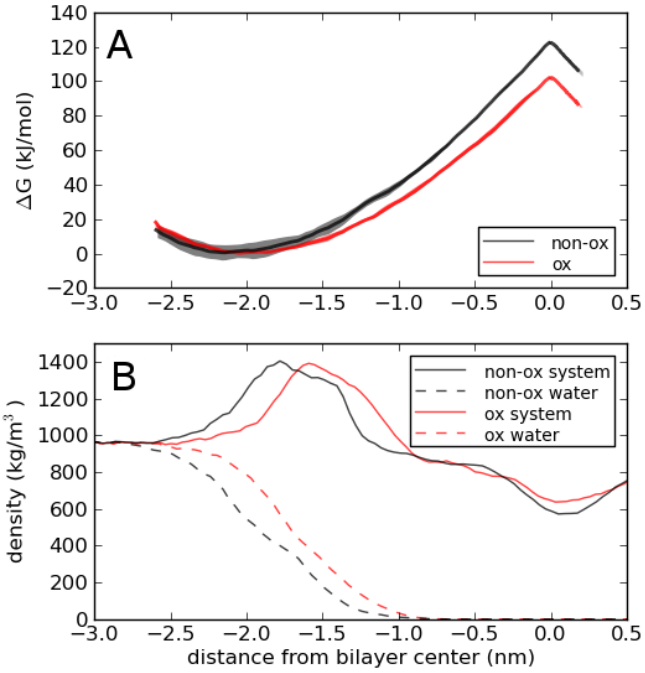
A
ΔG (kJ/mol)
non-ox
ox
B
density (kg/m^3)
non-ox system
non-ox water
ox system
ox water
distance from bilayer center (nm)

Figure 5